

Original Article



OPEN ACCESS

Received: Jan 5, 2022

Revised: Apr 26, 2022

Accepted: May 2, 2022

Published online: May 25, 2022

Address for Correspondence:

Muhannad A. Abbasi, MD

Department of Radiology, Feinberg School of Medicine, Northwestern University, 737 N Michigan Ave. (Suite 1600), Chicago, IL 60611, USA.

Email: muhannadaboudabbasi@gmail.com

Copyright © 2022 Korean Society of Echocardiography

This is an Open Access article distributed under the terms of the Creative Commons Attribution Non-Commercial License (<https://creativecommons.org/licenses/by-nc/4.0/>) which permits unrestricted non-commercial use, distribution, and reproduction in any medium, provided the original work is properly cited.

ORCID iDs

Muhannad A. Abbasi

<https://orcid.org/0000-0002-2774-542X>

Allison M. Blake

<https://orcid.org/0000-0003-2300-6299>

Allen S. Anderson

<https://orcid.org/0000-0001-7216-2613>

Jonathan D. Rich

<https://orcid.org/0000-0002-2370-5252>

Michael Markl

<https://orcid.org/0000-0002-7686-1128>

Funding

The work was supported by National Institutes of Health (National Heart, Lung, and Blood Institute [NHLBI] grant R01 HL117888).

Multiparametric Cardiac Magnetic Resonance Imaging Detects Altered Myocardial Tissue and Function in Heart Transplantation Recipients Monitored for Cardiac Allograft Vasculopathy

Muhannad A. Abbasi , MD¹, Allison M. Blake , MD¹, Roberto Sarnari, MD¹, Daniel Lee, MD¹, Allen S. Anderson , MD², Kambiz Ghafourian, MD², Sadiya S. Khan, MD², Esther E. Vorovich, MD², Jonathan D. Rich , MD², Jane E. Wilcox, MD², Clyde W. Yancy, MD², James C. Carr, MD¹, and Michael Markl , PhD¹

¹Department of Radiology, Feinberg School of Medicine, Northwestern University, Chicago, IL, USA

²Division of Cardiology, Department of Medicine, Northwestern University, Chicago, IL, USA

ABSTRACT

BACKGROUND: Cardiac allograft vasculopathy (CAV) is a complication beyond the first-year post-heart transplantation (HTx). We aimed to test the utility of cardiac magnetic resonance (CMR) to detect functional/structural changes in HTx recipients with CAV.

METHODS: Seventy-seven prospectively recruited HTx recipients beyond the first-year post-HTx and 18 healthy controls underwent CMR, including cine imaging of ventricular function and T1- and T2-mapping to assess myocardial tissue changes. Data analysis included quantification of global cardiac function and regional T2, T1 and extracellular volume based on the 16-segment model. International Society for Heart and Lung Transplantation criteria was used to adjudicate CAV grade (0–3) based on coronary angiography.

RESULTS: The majority of HTx recipients (73%) presented with CAV (1: n = 42, 2/3: n = 14, 0: n = 21). Global and segmental T2 (49.5 ± 3.4 ms vs 50.6 ± 3.4 ms, $p < 0.001$; 16/16 segments) were significantly elevated in CAV-0 compared to controls. When comparing CAV-2/3 to CAV-1, global and segmental T2 were significantly increased (53.6 ± 3.2 ms vs 50.6 ± 2.9 ms, $p < 0.001$; 16/16 segments) and left ventricular ejection fraction was significantly decreased ($54 \pm 9\%$ vs $59 \pm 9\%$, $p < 0.05$). No global, structural, or functional differences were seen between CAV-0 and CAV-1.

CONCLUSIONS: Transplanted hearts display functional and structural alteration compared to native hearts, even in those without evidence of macrovasculopathy (CAV-0). In addition, CMR tissue parameters were sensitive to changes in CAV-1 vs. 2/3 (mild vs. moderate/severe). Further studies are warranted to evaluate the diagnostic value of CMR for the detection and classification of CAV.

Keywords: Heart transplantation; Magnetic resonance imaging; Graft rejection; Coronary angiography

Conflict of Interest

The authors have no financial conflicts of interest.

Author Contributions

Conceptualization: Abbasi MA, Sarnari R, Wilcox JE, Yancy CW, Carr JC, Markl M; Data curation: Abbasi MA, Blake AM, Markl M; Formal analysis: Abbasi MA, Blake AM, Markl M; Funding acquisition: Carr JC, Markl M; Investigation: Blake AM, Sarnari R, Lee D, Markl M; Methodology: Sarnari R, Markl M; Resources: Markl M; Software: Blake AM; Supervision: Sarnari R, Lee D, Ghafourian K, Khan SS, Vorovich EE, Rich JD, Wilcox JE, Yancy CW, Carr JC, Markl M; Validation: Blake AM, Markl M; Visualization: Markl M; Writing - original draft: Abbasi MA, Blake AM, Markl M; Writing - review & editing: Abbasi MA, Blake AM, Sarnari R, Lee D, Anderson AS, Ghafourian K, Khan SS, Vorovich EE, Rich JD, Wilcox JE, Yancy CW, Carr JC, Markl M.

INTRODUCTION

Heart transplantation (HTx) is the procedure of choice for select patients with advanced heart failure refractory to medical management. Beyond the first year post-HTx, cardiac allograft vasculopathy (CAV) is one of the major complications limiting allograft health and longevity.¹⁻³⁾ The pathophysiology of CAV has not been completely elucidated.⁴⁾⁵⁾ However, it is proposed that immunological and vascular factors result in concentric fibromuscular intimal thickening that may affect the entire length of a vessel, in addition to atherosclerotic and vasculitic lesions.¹⁾⁴⁾ Furthermore, CAV can affect any vessel, from the epicardial vasculature to the intramuscular arteries, and microvascular bed, independently and unpredictably between patients.⁶⁾⁷⁾ Routine screening is recommended as HTx recipients may be asymptomatic or have non-specific symptoms secondary to allograft denervation.⁸⁾ Currently surveillance, diagnosis, and grading of CAV is performed with invasive coronary angiography (ICA), which has limited sensitivity in early disease⁹⁾¹²⁾ and may be associated with significant complication.¹³⁾

As a non-invasive diagnostic alternative, cardiac magnetic resonance (CMR) imaging has emerged as a promising tool for the assessment of global and regional changes in biventricular structure, function¹⁴⁾ and tissue characterization.¹⁵⁾ CMR cine imaging allows for assessment of global and regional changes in left ventricular (LV) structure and function, which has been validated in many cardiac conditions.¹⁶⁾ In addition, CMR tissue mapping techniques can be employed to detect changes in myocardial tissue, including myocardial fibrosis (evaluated with pre- and post-contrast T1-mapping to quantify extracellular volume [ECV] fraction)¹⁷⁾ and inflammation or edema (assessed by T2-mapping).¹⁸⁾

Our aim was to test the hypothesis that these multiparametric CMR techniques can non-invasively detect LV myocardial structural and functional changes for identification of CAV.

METHODS**Study cohort**

Eighty-three prospectively recruited HTx recipients beyond the first year post-HTx were initially identified as potential candidates for this study. Six patients were excluded from further analysis. Exclusion criteria included any patient who had not had undergone ICA ($n = 2$), a history of gadolinium (Gd) allergy, glomerular filtration rate < 30 mL/min, implanted foreign metal bodies, age < 18 , or an inability to obtain written consent ($n = 4$). Subsequently, 77 prospectively recruited HTx recipients beyond the first year post-HTx (51 ± 16 years, 44% female) and 18 matched controls (49 ± 15 years, 33% female) underwent CMR between November 2014 and October 2018. Eligible patients included any adult HTx recipient beyond the first year post-HTx who had also undergone routine clinical ICA for CAV surveillance. On average ICA was performed 0.6 ± 0.6 years from the time of CMR. If a patient received multiple CMR exams, the CMR scan most distant from the time of transplant was used as CAV is a progressive disease. Healthy controls underwent a non-contrast multi-parametric research CMR exam. The study was approved by the local institutional review board (IRB) (Northwestern University [NU] IRB STU00087510 Comprehensive Analysis in Heart Transplantation) and written informed consent was obtained from all participants.

CMR acquisition

All CMR studies were performed on a 1.5 Tesla MR-system (MAGNETOM Aera or Avanto; Siemens, Erlangen, Germany). Multiparametric CMR included retrospectively electrocardiographically gated 2-dimensional (2D) cine-steady state free precession (SSFP) imaging, T2-mapping, as well as pre-and post-Gd-contrast T1-mapping.

Cine-SSFP images of the entire heart were obtained in the short-axis (8–12 slices per stack) and the long-axis (2-chamber, 3-chamber and 4-chamber) orientations. Short-axis 2D cine-SSFP images covering the ventricles from base to apex were reconstructed to 25 cardiac time frames and acquired with the following imaging parameters: repetition time (TR) = 2.6–3.0 ms, echo time (TE) = 1.1–1.3 ms, flip angle = 50–87°, bandwidth/pixel = 930 Hz, Generalized Auto-calibrating Partially Parallel Acquisitions acceleration with R = 2, in-plane resolution = (1.5–2.3 mm)², slice thickness = 6–8 mm.

T2 and T1-mapping were acquired during breath-holding at 3 identical short-axis locations at the base, mid-ventricle, and apex. T1-mapping consisted of single-shot modified Look Locker inversion recovery (MOLLI) images before and 15 minutes following Gd contrast administration (Magnevist or Gadavist, 0.1 mmol/kg; Bayer, Leverkusen, Germany).¹⁹⁾ Pre- and post-Gd MOLLI sequences occurred in a 5(3)3 pattern over 11 heartbeats. Imaging parameters were as follows: TE/TR = 1.0–1.3 ms/2.5–4.2 ms, spatial resolution = 1.0–2.1 mm × 1.5–2.5 mm, slice thickness = 8 mm, flip angle = 35°. Imaging reconstruction included motion correction of the MOLLI images with different inversion times and the calculation of parametric LV T1-maps. T2-mapping was based on the successive acquisition of 3 T2-prepared SSFP images with varying T2 prep times (0, 24, 55 ms).¹⁸⁾ Further imaging parameters were as follows: TE = 1.1–1.4 ms, TR = 2.2–2.6 ms, spatial resolution = 1.5–2.1 mm × 2.0–2.5 mm, slice thickness = 8 mm, diastolic acquisition window = 270 ms, flip angle = 70°.

CMR post processing: global LV and RV function

Measures of global biventricular function were calculated from short-and long-axis cine SSFP images using commercial software (cvi42; Circle, Calgary, Canada). All volumetric measurements were indexed to body surface area (BSA). Measures of LV and right ventricle (RV) global function included LV/RV end-diastolic and end-systolic volumes (LVEDVI, LVESVI, RVEDVI, RVESVI), stroke volumes (LVSVI, RVSVI), ejection fractions (LVEF, RVEF), and LV end-diastolic myocardial-mass (LV-mass). Two physicians with 2 and 5 years of experience performed the post-processing segmentation and analysis.

CMR post processing: left ventricular T1, T2, and ECV

Global native T1 and T2 values were calculated from scanner-generated T2- and T1- (pre-and post- contrast) maps using commercial software (cvi42, v5.3.6; Circle). ECV was calculated during post-processing using pre-and post-Gd-contrast T1-maps and the patient's hematocrit level obtained the day of CMR using the equation: $ECV = (\Delta R1 \text{ Myocardium} / \Delta R1 \text{ Blood}) \times (1 - \text{Hematocrit})$, where $R1 = 1/T1$ and $\Delta R1$ is the change in relaxation rate between pre- and post-contrast images.²⁰⁾ For all regional analyses, the left ventricle was divided in 16 standardized segments based on the American Heart Association 16-segmental model.²¹⁾ Global (average of 16 segments) and peak (maximum segmental value out of 16 segments) T1, T2, and ECV values were derived from the 16-segment maps similar to previously reported strategies.²²⁾²³⁾ Two physicians with 2 and 5 years of experience performed the post-processing segmentation and analysis.

Invasive coronary angiography: CAV grading

HTx recipients underwent ICA using standard clinical protocols, with at least 2 projections obtained per coronary artery. The presence/absence, and degree of stenosis in the major epicardial coronary arteries were graded in a semi-quantitative fashion by visual analysis of 2 experienced cardiologists on an ordinal scale and applied to the International Society for Heart and Lung Transplantation (ISHLT) CAV classification.²⁴⁾ The ISHLT classification was used to categorize patients into different CAV grades (0-3). ISHLT CAV severity was determined by integrating degree of coronary stenosis and LVEF.²⁴⁾ The ICA performed closest to CMR was used for the final adjudication. Due to small cohort size, patients with CAV grade 2/3 were combined into one group.

Statistical analysis

All continuous data are presented as mean \pm standard deviation. Demographics, global function, global and segmental structural parameters (T1, T2, ECV) were compared between HTx recipients and to controls and amongst different CAV grades. Shapiro-Wilk tests were completed to assess for normality of the CMR parameters and Levene's tests were completed to assess the equality of variances between groups. Two-tailed independent t-tests or Mann-Whitney U tests were performed as appropriate for comparisons between 2 groups. One-way analysis of variance with Tukey tests for *post hoc* analysis or Kruskal-Wallis tests with Dunn's tests for *post hoc* analysis were used as appropriate to evaluate group differences across controls and CAV subgroups.

RESULTS

Study cohort

Seventy-seven HTx recipients beyond the first year post-HTx (51 \pm 16 years, 44% female) and 18 matched healthy controls (49 \pm 15 years, 33% female) were included in this study (Table 1). The average time of CMR was 9 \pm 6 years post-HTx with an average age at the CMR exam of 48 \pm 5.5

Table 1. Demographics and global biventricular functional parameters of controls and HTx recipients

Variables	Controls	All HTx recipients	CAV grade 0	CAV grade 1	CAV grade 2/3	p-value
Number of patients	18	77	21	42	14	N/A
Time from transplant (years)	N/A	9 \pm 6	8 \pm 5	9 \pm 6	11 \pm 7	0.280
Sex (Female)	6 (33)	34 (44)*	11 (52) [§]	20 (48)*	3 (25) ^{*†}	0.030
Age at scan (years)	49 \pm 15	51 \pm 16	48 \pm 16	54 \pm 17	46 \pm 14	0.460
BMI (kg/m ²)	29.1 \pm 4.5	28.0 \pm 5.5	25.4 \pm 4.3 ^{*†}	29.8 \pm 6.0 ^{†§}	26 \pm 2.9 ^{*†}	0.440
BSA (m ²)	1.9 \pm 0.2	2.0 \pm 0.3	1.8 \pm 0.2 ^{†§}	2.0 \pm 0.3 [†]	2.0 \pm 0.2 [†]	0.350
Systolic blood pressure (mmHg)	125 \pm 25	124 \pm 19	124 \pm 16	127 \pm 21	116 \pm 15	0.650
Diastolic blood pressure (mmHg)	72 \pm 18	77 \pm 11	76 \pm 10	79 \pm 11	74 \pm 11	0.110
Heart rate (bpm)	63 \pm 10	93 \pm 15	98 \pm 13*	89 \pm 15*	95 \pm 18*	< 0.001
LVEDVI (mL/m ²)	57 \pm 17	73 \pm 14*	57 \pm 8*	55 \pm 13*	64 \pm 29*	< 0.001
LVESVI (mL/m ²)	28 \pm 7	24 \pm 11	24 \pm 7*	22 \pm 7	31 \pm 21	0.200
LVSVI (mL/m ²)	45 \pm 9	35 \pm 10*	33 \pm 9*	33 \pm 6*	35 \pm 12*	< 0.001
LVEF (%)	62 \pm 5	58 \pm 9	58 \pm 9	59 \pm 9 [§]	54 \pm 9 ^{*†}	0.050
LV mass ED (g/m ²)	56 \pm 22	43 \pm 11*	42 \pm 11*	43 \pm 9*	45 \pm 17	< 0.001
RVEDVI (mL/m ²)	68 \pm 14	65 \pm 16	62 \pm 11	63 \pm 14	73 \pm 26	0.390
RVESVI (mL/m ²)	30 \pm 7	33 \pm 11	30 \pm 8	31 \pm 9	40 \pm 17	0.410
RVSVI (mL/m ²)	38 \pm 8	32 \pm 9*	32 \pm 7*	32 \pm 9	33 \pm 10	0.010
RVEF (%)	56 \pm 4	50 \pm 9*	52 \pm 10 [§]	51 \pm 9*	46 \pm 7 ^{*†}	0.008

BMI: body mass index, BSA: body surface area, CAV: cardiac allograft vasculopathy, ED: end diastole, EF: ejection fraction, EDVI: end-diastolic volume indexed to body surface area, ESVI: end-systolic volume indexed to body surface area, HTx: heart transplantation, LV: left ventricular, RV: right ventricle, SVI: stroke volume indexed to body surface area.

*Significance compared to controls; †Significance compared to CAV 0; ‡Significance compared to CAV 1; §Significance compared to CAV 2/3.

years. CAV grading by ICA revealed Twenty-one HTx recipients with CAV grade 0, 42 with CAV grade 1, and 14 with CAV grade 2/3. On average ICA was performed 0.6 ± 0.6 years from the time of CMR. There were more females in the HTx group compared to the control group (44% vs. 33%, $p = 0.03$), and fewer females in the CAV grade 2/3 group compared to CAV grade 0 cohort (25% vs. 52%, $p = 0.05$). HTx recipients with CAV grade 1 had significantly higher BMI than CAV grade 0 and CAV grade 2/3 (29.8 ± 6.0 kg/m² vs. 25.4 ± 4.3 kg/m², $p = 0.007$ and 26.0 ± 2.9 kg/m², $p = 0.02$). HTx recipients with CAV grade 1 and CAV grade 2/3 had significantly higher BSA than CAV grade 0 (2.0 ± 0.3 vs 1.8 ± 0.2 m², $p = 0.006$ and 2.0 ± 0.2 vs. 1.8 ± 0.2 m², $p = 0.05$).

Global LV and RV function

To account for differences in BMI all volumetric measurements were indexed to BSA. Compared to controls, HTx recipients had significantly reduced LVSVI, LVEF and RVEF ($p < 0.001$, $p = 0.05$, and $p = 0.008$, respectively). Between CAV subgroups, LVEF was significantly decreased among patients with CAV grade 2/3 compared to controls ($54 \pm 9\%$ vs. $62 \pm 5\%$, $p = 0.004$) and between CAV grade 2/3 compared to CAV grade 1 ($54 \pm 9\%$ vs. $59 \pm 9\%$, $p = 0.02$). RVEF was also significantly lower in patients with CAV grade 2/3 compared to controls ($46 \pm 7\%$ vs. $56 \pm 4\%$, $p < 0.001$), and CAV grade 2/3 compared to CAV grade 0 ($46 \pm 7\%$ vs. $52 \pm 10\%$, $p = 0.03$). To account for differences in BMI between the control group and HTx recipients an additional analysis was performed using values indexed to BSA for all volumetric measurements LVSV indexed and RVSV indexed was significantly decreased between all CAV groups (grade 0–3) and controls **Table 1** ($p < 0.001$ and $p = 0.01$).

T2, T1 and ECV-mapping

Figure 1 shows representative LV short axis ECV and T2 maps in a healthy control and HTx recipients of different CAV subgroups. For both tissue parameters, the maps show increased T2 and ECV in HTx recipients compared to controls for all CAV grades 0–3. In addition, increasing CAV grade resulted in increasing T2 and ECV. These findings are corroborated by the results across all HTx groups.

As shown in **Table 2**, peak T1 was significantly elevated in all HTx recipients compared to controls ($1,107 \pm 74$ ms vs. $1,072 \pm 50$ ms, $p = 0.05$), and when comparing CAV grade 0 to CAV grade 2/3 ($1,081 \pm 32$ ms vs. $1,130 \pm 79$ ms, $p = 0.03$). On a segmental level, T1 was significantly elevated in 7/16 segments between HTx recipients and healthy controls (**Figure 2**). When comparing subgroups, T1 was significantly elevated in 2/16 segments between CAV grade 0 and controls, and 1 segment between CAV grade 2/3 and CAV grade 1 (**Figure 3**).

Global ECV ($27.6 \pm 3.7\%$ vs. $25.1 \pm 3.4\%$, $p = 0.004$) and peak ECV ($32.1 \pm 4.3\%$ vs. $28.6 \pm 3.8\%$, $p < 0.001$) were significantly elevated in the entire cohort of HTx recipients compared to controls (**Table 2**). Segmentally, ECV was significantly elevated in 7/16 segments for HTx recipients vs. healthy controls (**Figure 2**), and in 2/16 segments between CAV grade 1 and CAV grade 2/3 (**Figure 3**).

Global T2 (50.6 ± 3.4 ms vs. 45.5 ± 2.1 ms, $p < 0.001$) and peak T2 (56.6 ± 8.2 ms vs. 50.0 ± 2.4 ms, $p < 0.001$) were significantly elevated in the entire HTx cohort compared to controls (**Table 2**). Additionally, global T2 was significantly increased in CAV 2/3 compared to CAV 0 and CAV 1 (53.6 ± 3.2 vs. 49.5 ± 3.4 , $p = 0.001$ and 50.6 ± 2.9 , $p = 0.02$; **Table 2**). Segmental T2 was significantly elevated across all 16 LV segments in HTx recipients when compared to healthy controls (**Figure 2**). On subgroup analysis, 16/16 segments were elevated when comparing CAV grade 0 to healthy controls (**Figure 3**). Additionally, 6/16 segments had

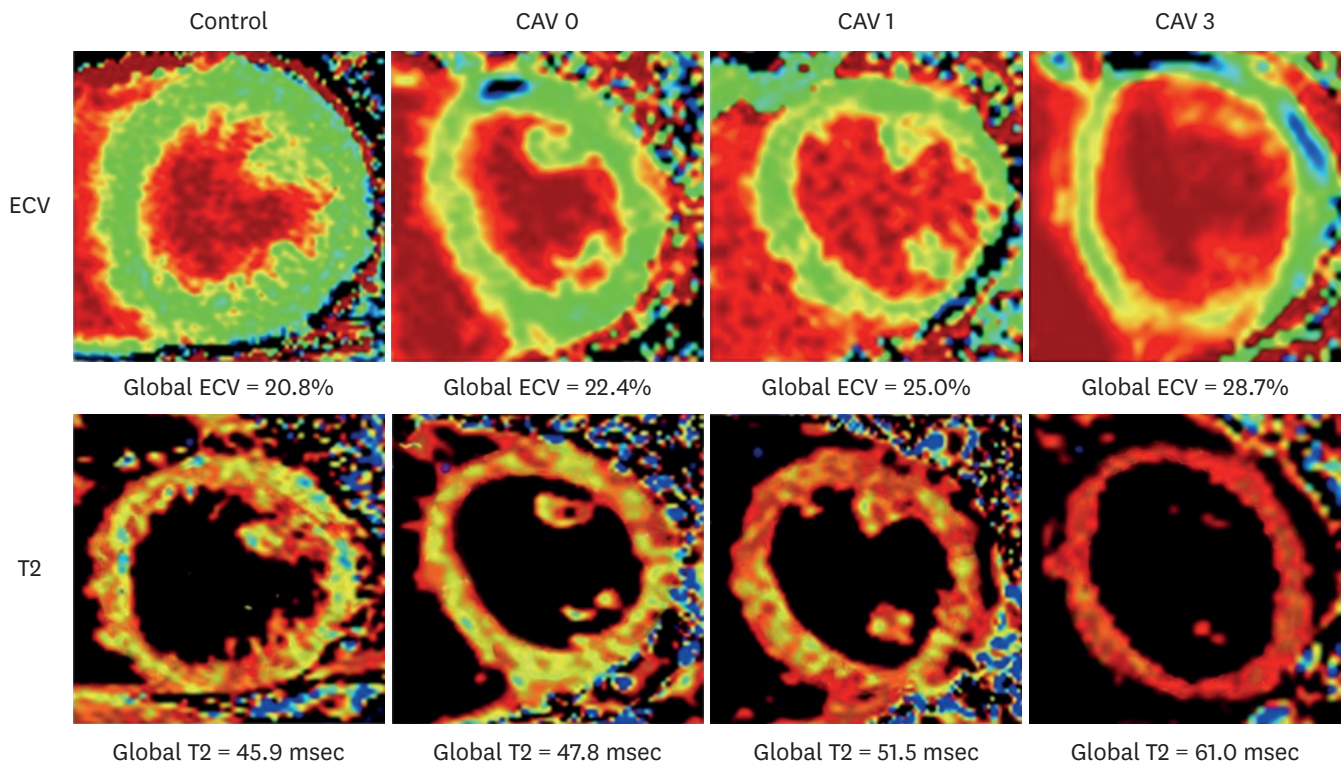


Figure 1. T2 and ECV maps in a healthy control and heart transplantation recipient representative of the different CAV subgroups. CAV: cardiac allograft vasculopathy, ECV: extracellular volume.

Table 2. Global structural and peak structural parameters for controls and CAV subgroups

Variables	Controls	All HTx recipients	CAV 0	CAV 1	CAV 2/3	p-value
T1 (ms)						
Global	1,000 ± 33	1,027 ± 57	1,020 ± 62	1,028 ± 58	1,031 ± 51	0.070
Peak	1,072 ± 50	1,107 ± 74*	1,081 ± 32 [§]	1,113 ± 76*	1,130 ± 79* [†]	0.050
ECV (%)						
Global	25.1 ± 3.4	27.6 ± 3.7*	26.8 ± 4.6	27.2 ± 2.7*	29.0 ± 4.9*	0.004
Peak	28.6 ± 3.8	32.1 ± 4.3*	32.0 ± 5.0*	32.0 ± 3.7*	32.8 ± 5.2*	< 0.001
T2 (ms)						
Global	45.5 ± 2.1	50.6 ± 3.4*	49.5 ± 3.4* [§]	50.6 ± 2.9* [§]	53.6 ± 3.2* ^{††}	< 0.001
Peak	50.0 ± 2.4	56.6 ± 8.2*	55.6 ± 3.4* [§]	57.0 ± 5.1*	56.5 ± 16.9* [†]	< 0.001

CAV: cardiac allograft vasculopathy, HTx: heart transplantation, ECV: extracellular volume.

*Significance compared to controls; [†]Significance compared to CAV 0; [§]Significance compared to CAV 1; ^{††}Significance compared to CAV 2/3.

significantly elevated T2 values when comparing CAV grade 2/3 to CAV grade 1 (**Figure 3**). Only one segment was significantly elevated in CAV grade 1 vs. CAV grade 0 (**Figure 3**).

DISCUSSION

In this study, CMR was applied as a noninvasive method of interrogating global and segmental cardiac structure and function in a cohort of patients monitored for CAV beyond the first year post-HTx. Our main findings include (1) Global T2 and ECV, and segmental T1, T2, and ECV values were significantly elevated between HTx recipients and controls; (2) HTx recipients with no evidence of CAV (CAV grade 0) had significantly elevated peak T2 and ECV when compared to healthy controls; (3) Global and segmental T2 and LVEF were significantly different between CAV grade 2/3 and CAV grade 1.

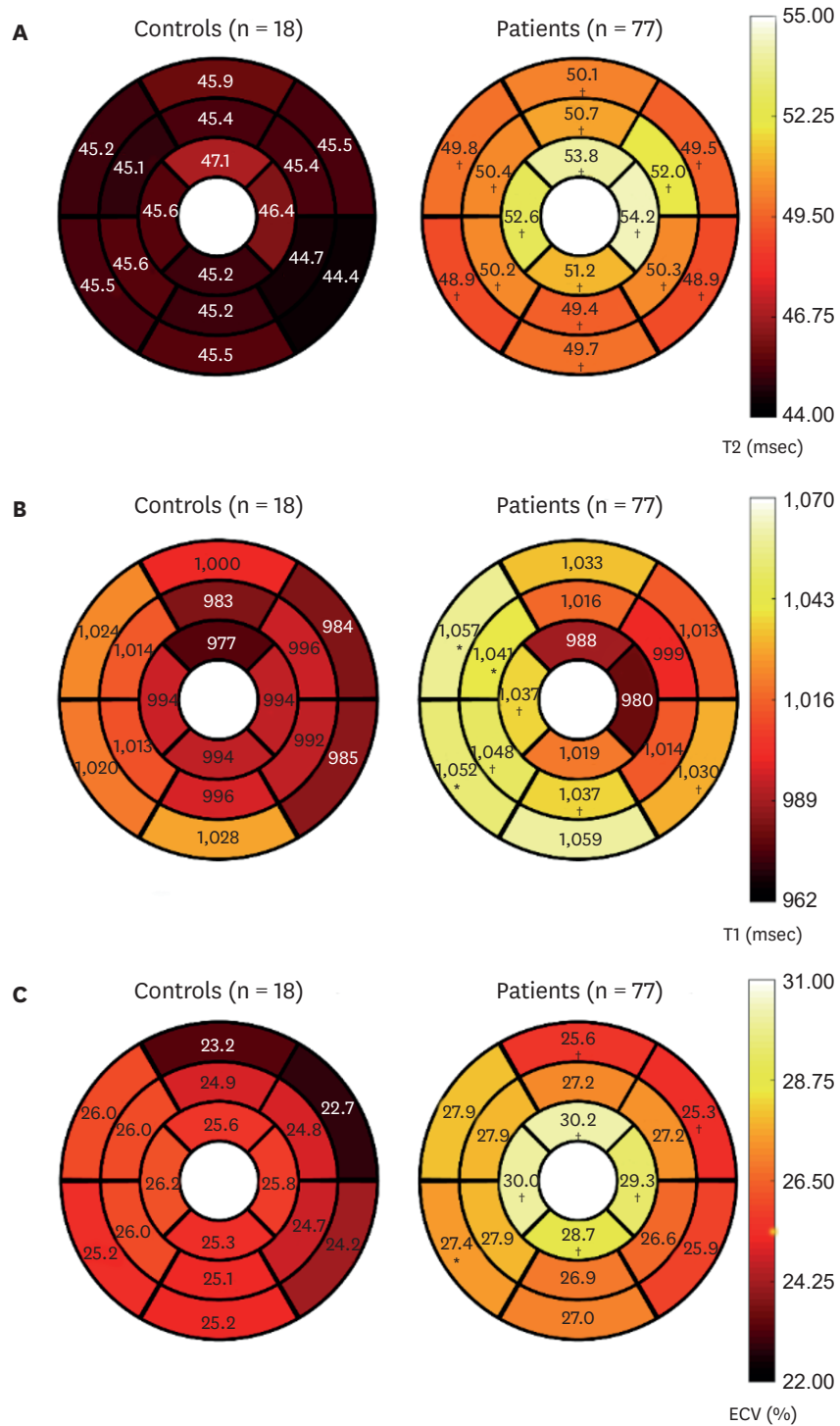


Figure 2. LV segmental comparison of T2 (A), T1 (B) and ECV (C) values between controls and heart transplantation recipients. The bull-eye plots show T2, T1 and ECV across the 16 American Heart Association LV segments.

ECV: extracellular volume, LV: left ventricular.

Significant differences are denoted by * $p < 0.05$ and † $p < 0.001$.

Prior studies in HTx recipients have shown similar differences in T1, T2, and ECV when compared to controls. Our group has previously reported increased T1 and T2 values in

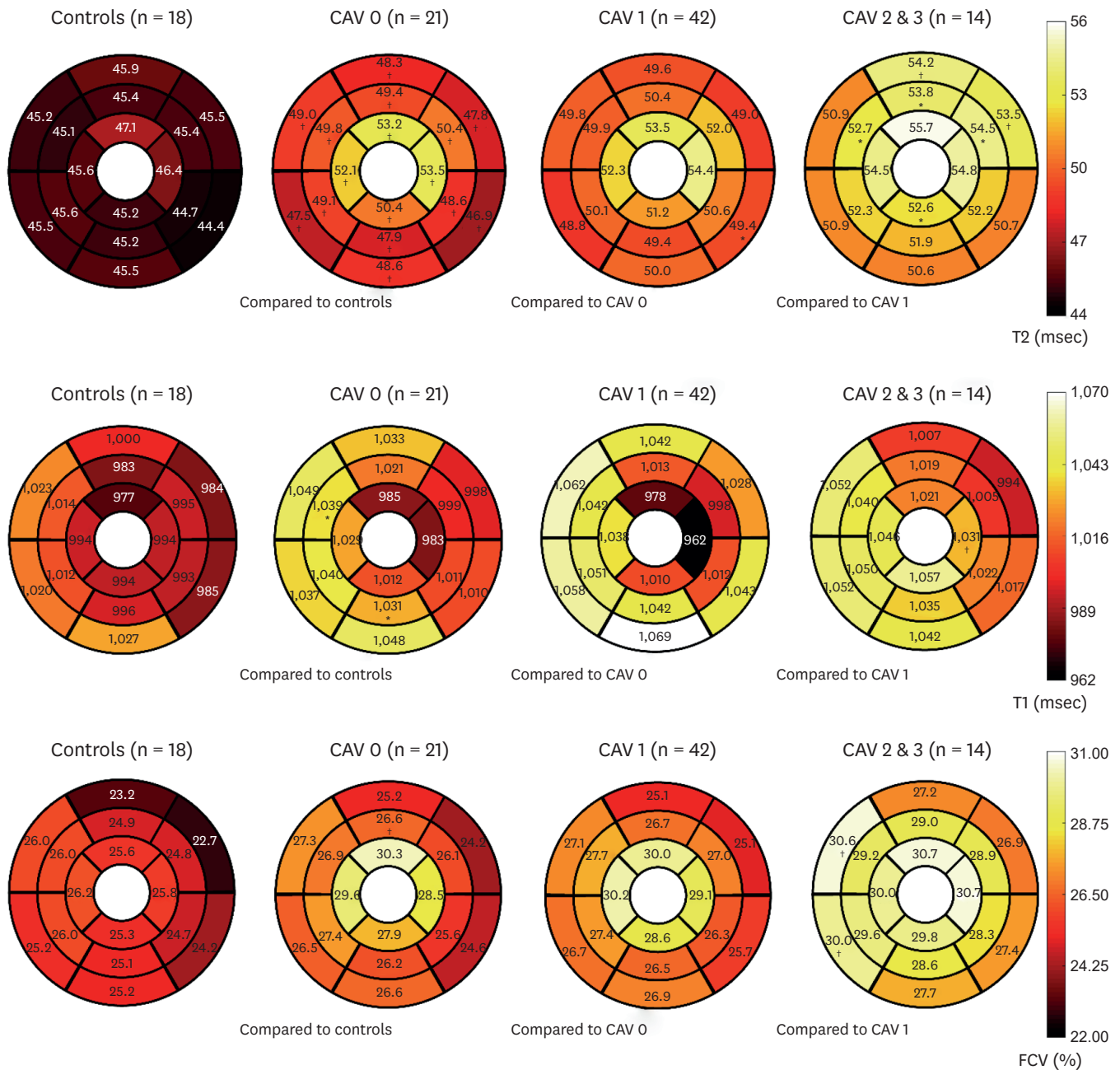


Figure 3. LV segmental comparison of T2, T1 and ECV between controls and CAV subgroups. The bull-eye plots show T2, T1 and ECV across the 16 American Heart Association LV + RV segments. CAV: cardiac allograft vasculopathy, ECV: extracellular volume, LV: left ventricular, RV: right ventricle. Significant differences are denoted by *p < 0.05 and †p < 0.001.

HTx patients compared to healthy controls, which may persist beyond the first year post-HTx.²²⁾²³⁾²⁵⁾ In our study the lack of differences in global T1 values between controls and all CAV subgroups may suggest that fibrosis is not the main driver of the functional changes. Yuan et al.²⁶⁾ showed elevated ECV and T2 in HTx recipients when compared to controls, hypothesizing that myocardial edema may be a contributor to ECV expansion following heart transplant. ECV expansion could explain why even HTx recipients without vasculopathy (CAV grade 0) had elevated ECV and T2 when compared to controls.

The lack of difference in T2 between CAV grade 0 and CAV grade 1 could be related to the CAV grading criteria. CAV grade 0 is assigned when there is no coronary disease present, while CAV grade 1 is assigned when there is < 50% stenosis of the left main coronary artery, or < 70% stenosis of the other primary or branch vessels. These CAV grade 1 lesions may thus not be physiologically significant (for example a 10% left main stenosis) or too early in the disease process to have caused detectable myocardial changes above and beyond what is caused by microvascular disease. Differences between CAV grade 1 and CAV grade 2/3, on the other hand, demonstrate the progressive nature of the disease process with greater degrees of stenosis causing significant myocardial disease detectable by T2 mapping. This is further demonstrated by the reduction of LVEF seen in CAV grade 2/3 when compared to CAV grade 1.

Transplanted hearts display functional and structural alteration compared to native hearts, even in those without evidence of macrovasculopathy (CAV grade 0). This may indicate a subclinical disease process such as rejection, infection or microvasculopathy. CMR-based myocardial perfusion assessment suggests that CAV grading by angiography may be underestimating the degree of vasculopathy and may this be unreliable to detect microvascular disease.²⁷⁻²⁹⁾ There have been estimates that up to 20% of patients with no angiographically detectable vasculopathy have abnormal CMR-perfusion imaging.³⁰⁻³¹⁾ Braggion-Santos et al.³²⁾ studied late gadolinium enhancement (LGE) in HTx recipients and found that 19% of patients with CAV grade 0 had infarct pattern-LGE lesions. The authors hypothesize that the cause is likely 2-fold. First, there are primarily intramural inflammatory/atherosclerotic lesions which may not cause angiographically significant stenosis until later in the disease process, and second, there may be microvascular disease which is not evaluated in conventional angiography.³³⁾ A further study conducted by Chih et al.²⁸⁾ demonstrated that a CMR-myocardial perfusion reserve of ≤ 1.68 had a negative predictive value of 100%, suggesting its potential as a test to rule out CAV. In recent pooled analysis of 8 studies (implementing some form of CMR derived myocardial perfusion reserve strain or index), CMR had a sensitivity range from 41-100% and specificity range from 61-100% in detecting CAV.³⁴⁾

While our study focused on using CMR based techniques to assess for changes related to CAV, it is important to note that several other non-invasive techniques have been studied to assess, detect and quantify CAV in HTx recipients.³⁴⁻³⁵⁾ Stress echocardiography (STE), for example, is an option for patients that cannot undergo invasive angiography (due to renal function, unacceptably high risk of heart catheterization).³⁶⁾ However, a recent meta-analysis cited a sensitivity of only 60% in the detection of CAV, with a specificity of 86%.³⁷⁾ Multiple other studies have demonstrated that STE is not able to detect mild or moderate CAV in the first 5 years after HTx,³⁸⁻⁴⁰⁾ however, does have a sensitivity of up to 80% to detect severe CAV.³⁹⁾ The sensitivity of STE is enhanced when combined with strain imaging assessing myocardial deformation and coronary flow velocity reversal.⁴¹⁻⁴²⁾ Coronary CT angiography (CCTA) has emerged as a powerful tool which is able to delineate coronary wall change associated with CAV, as well as degree of stenosis. Usually, the utility of CCTA is limited by elevated resting heart rates of a denervated allograft, and the use of nephrotoxic iodinated contrast.⁴³⁾ However, advancements in techniques (i.e., dual source, multi-segment reconstruction and motion correct algorithms) render CCTA appealing, particularly with the ability to detect an intimal maximal thickness > 0.5 mm with the same sensitivity as intravascular ultrasonography. These advances make CCTA more sensitive than ICA in some ways, particularly with the specific pathophysiology of CAV in mind.⁴⁴⁾ A recent pooled analysis of 24 studies reported that the sensitivity of CCTA ranged from 70-100% associated with a specificity ranging from 75-100%.³⁴⁾

CCTA with measurement of the fractional flow is able to show coronary wall change of CAV as well as degree of stenosis noninvasively with a recent meta-analysis of 13 studies (n = 615) showed that CTA and angiography were able to detect CAV and significant CAV (stenosis \geq 50%) with mean sensitivities of 97% and 94%, specificities of 81% and 92%.⁴⁵⁾ Stress perfusion CT may allow for the detection of perfusion change in LV myocardium of patients with CAV.⁴⁶⁾ Finally, the coronary artery calcium (CAC) score seems to be of particular interest as recent prospective study including 113 transplant recipients cited an overall sensitivity of 88% and negative predictive value of 97% for CAC in detecting CAV 2–3 (moderate-severe CAV).⁴⁷⁾

Limitations of our study include (1) We did not assess microvascular disease (or a surrogate) which may have helped confirm our hypothesis that the lack of differences of structural and functional differences between CAV grade 0 and grade 1 may indicate underlying microvasculopathy. (2) We assessed structural parameters (T2, T1, and ECV) and functional parameters (biventricular ejection fraction), and acknowledge that the inclusion of further myocardial strain based functional assessment using magnetic resonance (MR) tagging techniques,⁴⁸⁾ or using DENSE⁴⁹⁾ may allow for a quantitative comparison between global and regional MR functional measures in this cohort. (3) Only LV structural parameters were studied.

In conclusion, differences in structural and functional parameters in HTx recipients with CAV grade 1 versus CAV grade 2/3 illustrate the potential of CMR to non-invasively detect progressive myocardial tissue and function changes associated with CAV severity. Additionally, detection of structural differences in HTx grafts that do not have angiographically detectable disease support the usefulness of CMR in non-invasive monitoring of patients following HTx as an adjunct to ICA. Future work should include assessment of the microvascular component of CAV to further assess value and feasibility of multiparametric CMR as a non-invasive screening tool for patients monitored for CAV.

REFERENCES

1. Lee MS, Tadwalkar RV, Fearon WF, et al. Cardiac allograft vasculopathy: a review. *Catheter Cardiovasc Interv* 2018;92:E527-36.
[PUBMED](#) | [CROSSREF](#)
2. Lund LH, Khush KK, Cherikh WS, et al. The registry of the International Society for Heart and Lung Transplantation: Thirty-fourth Adult Heart Transplantation Report-2017; Focus theme: allograft ischemic time. *J Heart Lung Transplant* 2017;36:1037-46.
[PUBMED](#) | [CROSSREF](#)
3. Yusen RD, Edwards LB, Dipchand AI, et al. The registry of the International Society for Heart and Lung Transplantation: Thirty-third Adult Lung and Heart-Lung Transplant Report-2016; Focus theme: primary diagnostic indications for transplant. *J Heart Lung Transplant* 2016;35:1170-84.
[PUBMED](#) | [CROSSREF](#)
4. Lee F, Nair V, Chih S. Cardiac allograft vasculopathy: insights on pathogenesis and therapy. *Clin Transplant* 2020;34:e13794.
[PUBMED](#) | [CROSSREF](#)
5. Lu WH, Palatnik K, Fishbein GA, et al. Diverse morphologic manifestations of cardiac allograft vasculopathy: a pathologic study of 64 allograft hearts. *J Heart Lung Transplant* 2011;30:1044-50.
[PUBMED](#) | [CROSSREF](#)
6. Abu-Qaoud MS, Stoletniy LN, Chen D, Kerstetter J, Kuhn M, Pai RG. Lack of relationship between microvascular and macrovascular disease in heart transplant recipients. *Transplantation* 2012;94:965-70.
[PUBMED](#) | [CROSSREF](#)
7. Kübrich M, Petrakopoulou P, Kofler S, et al. Impact of coronary endothelial dysfunction on adverse long-term outcome after heart transplantation. *Transplantation* 2008;85:1580-7.
[PUBMED](#) | [CROSSREF](#)

8. Awad M, Czer LS, Hou M, et al. Early denervation and later reinnervation of the heart following cardiac transplantation: a review. *J Am Heart Assoc* 2016;5:e004070.
[PUBMED](#) | [CROSSREF](#)
9. Gao SZ, Alderman EL, Schroeder JS, Hunt SA, Wiederhold V, Stinson EB. Progressive coronary luminal narrowing after cardiac transplantation. *Circulation* 1990;82:IV269-75.
[PUBMED](#)
10. Sharples LD, Jackson CH, Parameshwar J, Wallwork J, Large SR. Diagnostic accuracy of coronary angiography and risk factors for post-heart-transplant cardiac allograft vasculopathy. *Transplantation* 2003;76:679-82.
[PUBMED](#) | [CROSSREF](#)
11. St Goar FG, Pinto FJ, Alderman EL, et al. Detection of coronary atherosclerosis in young adult hearts using intravascular ultrasound. *Circulation* 1992;86:756-63.
[PUBMED](#) | [CROSSREF](#)
12. Pollack A, Nazif T, Mancini D, Weisz G. Detection and imaging of cardiac allograft vasculopathy. *JACC Cardiovasc Imaging* 2013;6:613-23.
[PUBMED](#) | [CROSSREF](#)
13. Ricci MA, Trevisani GT, Pilcher DB. Vascular complications of cardiac catheterization. *Am J Surg* 1994;167:375-8.
[PUBMED](#) | [CROSSREF](#)
14. Tadic M. Multimodality evaluation of the right ventricle: an updated review. *Clin Cardiol* 2015;38:770-6.
[PUBMED](#) | [CROSSREF](#)
15. Ferreira VM, Piechnik SK, Robson MD, Neubauer S, Karamitsos TD. Myocardial tissue characterization by magnetic resonance imaging: novel applications of T1 and T2 mapping. *J Thorac Imaging* 2014;29:147-54.
[PUBMED](#) | [CROSSREF](#)
16. Puntmann VO, Valbuena S, Hinojar R, et al. Society for Cardiovascular Magnetic Resonance (SCMR) expert consensus for CMR imaging endpoints in clinical research: part I - analytical validation and clinical qualification. *J Cardiovasc Magn Reson* 2018;20:67.
[PUBMED](#) | [CROSSREF](#)
17. Moon JC, Messroghli DR, Kellman P, et al. Myocardial T1 mapping and extracellular volume quantification: a Society for Cardiovascular Magnetic Resonance (SCMR) and CMR Working Group of the European Society of Cardiology consensus statement. *J Cardiovasc Magn Reson* 2013;15:92.
[PUBMED](#) | [CROSSREF](#)
18. Giri S, Chung YC, Merchant A, et al. T2 quantification for improved detection of myocardial edema. *J Cardiovasc Magn Reson* 2009;11:56.
[PUBMED](#) | [CROSSREF](#)
19. Messroghli DR, Radjenovic A, Kozierke S, Higgins DM, Sivanathan MU, Ridgway JP. Modified Look-Locker inversion recovery (MOLLI) for high-resolution T1 mapping of the heart. *Magn Reson Med* 2004;52:141-6.
[PUBMED](#) | [CROSSREF](#)
20. Haaf P, Garg P, Messroghli DR, Broadbent DA, Greenwood JP, Plein S. Cardiac T1 mapping and extracellular volume (ECV) in clinical practice: a comprehensive review. *J Cardiovasc Magn Reson* 2017;18:89.
[PUBMED](#) | [CROSSREF](#)
21. Cerqueira MD, Weissman NJ, Dilsizian V, et al. Standardized myocardial segmentation and nomenclature for tomographic imaging of the heart. A statement for healthcare professionals from the Cardiac Imaging Committee of the Council on Clinical Cardiology of the American Heart Association. *Circulation* 2002;105:539-42.
[PUBMED](#) | [CROSSREF](#)
22. Dolan RS, Rahsepar AA, Blaisdell J, et al. Cardiac structure-function MRI in patients after heart transplantation. *J Magn Reson Imaging* 2019;49:678-87.
[PUBMED](#) | [CROSSREF](#)
23. Dolan RS, Rahsepar AA, Blaisdell J, et al. Multiparametric cardiac magnetic resonance imaging can detect acute cardiac allograft rejection after heart transplantation. *JACC Cardiovasc Imaging* 2019;12:1632-41.
[PUBMED](#) | [CROSSREF](#)
24. Mehra MR, Crespo-Leiro MG, Dipchand A, et al. International Society for Heart and Lung Transplantation working formulation of a standardized nomenclature for cardiac allograft vasculopathy-2010. *J Heart Lung Transplant* 2010;29:717-27.
[PUBMED](#) | [CROSSREF](#)
25. Markl M, Rustogi R, Galizia M, et al. Myocardial T2-mapping and velocity mapping: changes in regional left ventricular structure and function after heart transplantation. *Magn Reson Med* 2013;70:517-26.
[PUBMED](#) | [CROSSREF](#)

26. Yuan Y, Cai J, Cui Y, et al. CMR-derived extracellular volume fraction (ECV) in asymptomatic heart transplant recipients: correlations with clinical features and myocardial edema. *Int J Cardiovasc Imaging* 2018;34:1959-67.
[PUBMED](#) | [CROSSREF](#)
27. Miller CA, Sarma J, Naish JH, et al. Multiparametric cardiovascular magnetic resonance assessment of cardiac allograft vasculopathy. *J Am Coll Cardiol* 2014;63:799-808.
[PUBMED](#) | [CROSSREF](#)
28. Chih S, Ross HJ, Alba AC, Fan CS, Manlhiot C, Crean AM. Perfusion cardiac magnetic resonance imaging as a rule-out test for cardiac allograft vasculopathy. *Am J Transplant* 2016;16:3007-15.
[PUBMED](#) | [CROSSREF](#)
29. Erbel C, Mukhammadaminova N, Gleissner CA, et al. Myocardial perfusion reserve and strain-encoded CMR for evaluation of cardiac allograft microvasculopathy. *JACC Cardiovasc Imaging* 2016;9:255-66.
[PUBMED](#) | [CROSSREF](#)
30. Korosoglou G, Osman NF, Dengler TJ, et al. Strain-encoded cardiac magnetic resonance for the evaluation of chronic allograft vasculopathy in transplant recipients. *Am J Transplant* 2009;9:2587-96.
[PUBMED](#) | [CROSSREF](#)
31. Korosoglou G, Riedle N, Erbacher M, et al. Quantitative myocardial blush grade for the detection of cardiac allograft vasculopathy. *Am Heart J* 2010;159:643-651.e2.
[PUBMED](#) | [CROSSREF](#)
32. Braggion-Santos MF, Lossnitzer D, Buss S, et al. Late gadolinium enhancement assessed by cardiac magnetic resonance imaging in heart transplant recipients with different stages of cardiac allograft vasculopathy. *Eur Heart J Cardiovasc Imaging* 2014;15:1125-32.
[PUBMED](#) | [CROSSREF](#)
33. van Heeswijk RB, Bastiaansen JA, Iglesias JF, et al. Quantification of myocardial interstitial fibrosis and extracellular volume for the detection of cardiac allograft vasculopathy. *Int J Cardiovasc Imaging* 2020;36:533-42.
[PUBMED](#) | [CROSSREF](#)
34. Ajluni SC Jr, Mously H, Chami T, et al. Non-invasive imaging in the evaluation of cardiac allograft vasculopathy in heart transplantation: a systematic review. *Curr Probl Cardiol* 2022;101103.
[PUBMED](#) | [CROSSREF](#)
35. Sciacaluga C, Ghionzoli N, Mandoli GE, et al. The role of non-invasive imaging modalities in cardiac allograft vasculopathy: an updated focus on current evidences. *Heart Fail Rev* 2021 Aug 12 [E-pub ahead of print], <https://doi.org/10.1007/s10741-021-10155-0>.
[PUBMED](#) | [CROSSREF](#)
36. Costanzo MR, Dipchand A, Starling R, et al. The International Society of Heart and Lung Transplantation guidelines for the care of heart transplant recipients. *J Heart Lung Transplant* 2010;29:914-56.
[PUBMED](#) | [CROSSREF](#)
37. Elkaryoni A, Abu-Sheasha G, Altibi AM, Hassan A, Ellakany K, Nanda NC. Diagnostic accuracy of dobutamine stress echocardiography in the detection of cardiac allograft vasculopathy in heart transplant recipients: a systematic review and meta-analysis study. *Echocardiography* 2019;36:528-36.
[PUBMED](#) | [CROSSREF](#)
38. Clerkin KJ, Ali ZA, Mancini DM. New developments for the detection and treatment of cardiac vasculopathy. *Curr Opin Cardiol* 2017;32:316-25.
[PUBMED](#) | [CROSSREF](#)
39. Clerkin KJ, Farr MA, Restaino SW, Ali ZA, Mancini DM. Dobutamine stress echocardiography is inadequate to detect early cardiac allograft vasculopathy. *J Heart Lung Transplant* 2016;35:1040-1.
[PUBMED](#) | [CROSSREF](#)
40. Akosah KO, Mohanty PK, Funai JT, et al. Noninvasive detection of transplant coronary artery disease by dobutamine stress echocardiography. *J Heart Lung Transplant* 1994;13:1024-38.
[PUBMED](#)
41. Masarone D, Kittleson M, Gravino R, Valente F, Petraio A, Pacileo G. The role of echocardiography in the management of heart transplant recipients. *Diagnostics (Basel)* 2021;11:2338.
[PUBMED](#) | [CROSSREF](#)
42. Clemmensen TS, Eiskjær H, Løgstrup BB, Ilkjær LB, Poulsen SH. Left ventricular global longitudinal strain predicts major adverse cardiac events and all-cause mortality in heart transplant patients. *J Heart Lung Transplant* 2017;36:567-76.
[PUBMED](#) | [CROSSREF](#)
43. Poher JS, Chih S, Kobashigawa J, Madsen JC, Tellides G. Cardiac allograft vasculopathy: current review and future research directions. *Cardiovasc Res* 2021;117:2624-38.
[PUBMED](#) | [CROSSREF](#)

44. Schepis T, Achenbach S, Weyand M, et al. Comparison of dual source computed tomography versus intravascular ultrasound for evaluation of coronary arteries at least one year after cardiac transplantation. *Am J Cardiol* 2009;104:1351-6.
[PUBMED](#) | [CROSSREF](#)
45. Shah NR, Blankstein R, Villines T, Imran H, Morrison AR, Cheezum MK. Coronary CTA for surveillance of cardiac allograft vasculopathy. *Curr Cardiovasc Imaging Rep* 2019;12:1-7.
[PUBMED](#) | [CROSSREF](#)
46. Oebel S, Hamada S, Higashigaito K, et al. Comprehensive morphologic and functional imaging of heart transplant patients: first experience with dynamic perfusion CT. *Eur Radiol* 2018;28:4111-21.
[PUBMED](#) | [CROSSREF](#)
47. Günther A, Andersen R, Gude E, et al. The predictive value of coronary artery calcium detected by computed tomography in a prospective study on cardiac allograft vasculopathy in heart transplant patients. *Transpl Int* 2018;31:82-91.
[PUBMED](#) | [CROSSREF](#)
48. Zerhouni EA, Parish DM, Rogers WJ, Yang A, Shapiro EP. Human heart: tagging with MR imaging--a method for noninvasive assessment of myocardial motion. *Radiology* 1988;169:59-63.
[PUBMED](#) | [CROSSREF](#)
49. Aletras AH, Ding S, Balaban RS, Wen H. DENSE: displacement encoding with stimulated echoes in cardiac functional MRI. *J Magn Reson* 1999;137:247-52.
[PUBMED](#) | [CROSSREF](#)